Trinity College Dublin
Coláiste na Tríonóide, Baile Átha Cliath
The University of Dublin

School of Physics

Coulomb Crystals

An Investigation into the Equilibrium States of Ions Confined to Two Dimensions

Isabelle Heuzé

Supervisor: Prof. Stefan Hutzler

March 2023

A dissertation submitted in partial fulfilment of the requirements for the degree of B.A. of Theoretical Physics

Abstract

This project investigated the equilibrium states of ten identical ions confined to two dimensions by a Penning trap. Through computer simulation, the positions of ions in equilibrium were identified and the resulting structures were analysed using energy measurements and techniques such as Average Nearest Neighbour distances, Voronoi Entropy, and Radial Distribution Functions. We found a strong correlation between the energy and the average nearest neighbour distance of a structure. However, whilst further analysis suggested the possibility of correlations between other variables, it did not reveal any definite relationships. These findings contribute to our understanding of ion confinement in two dimensions and provide insight into the behaviour of similar systems in the future.

Acknowledgements

I would like to thank my supervisor, Prof. Stefan Hutzler, as well as Dr. Adil Mughal, and Prof. Denis Weaire for helping me with this project and for all the advice, support, and comments I've been given during the year. I was given a program on how to find the coordinates of structures by Dr. Adil Mughal, University of Aberystwyth, Wales. The analysis of them, I completed myself.

Contents

List of Figures

1. Introduction

This study focuses on the structures of 2D Coulomb crystals, which are systems of identical ions that are confined to two dimensions in two orthogonal directions by transverse harmonic potentials and interact with one another via a Coulomb potential [1, 2]. There have been a limited number of attempts to computationally describe and enumerate the equilibrium states of these ions [1, 3]. These previous computational efforts have characterised these structures using energy as the main measure of characterisation, but there are other techniques that have yet to be explored. Our study aims to address this gap in knowledge by investigating equilibrium states for crystals with 10 ions and analysing their configurations using energy as well as the techniques of Nearest Neighbours, Voronoi Entropy (see Section 2.3), Radial Distribution Functions (see Section 2.4), and distance matrices.

The motivation behind investigating 2D Coulomb Crystals is the applications offered in quantum computing [4, 5]. A quantum computer can be implemented with cold ions confined in a linear trap and interacting with laser control fields. Quantum gates involving any subset of ions can be realised by coupling the ions through the collective quantized motion [4]. The coupling of the internal states to the motion of the ions transverse to the crystal plane allows one to implement two-qubit quantum gates, which are the building blocks of quantum circuits. Very high gate fidelities can be achieved with this setup [5], meaning it is close to the ideal case. This study seeks to contribute to a deeper understanding of these structures and their potential applications in the field of quantum computing. By understanding the relationships between variables such as energy, symmetry, and uniformity, researchers can optimise the performance of Coulomb crystal based quantum computing systems.

2. Ions Confined to Two Dimensions

Each structure described in this study is an equilibrium configuration of a number of ions. A harmonic potential is applied to bring a system of identical ions together and confine them to two dimensions; these ions interact with each other via a Coulomb potential which repels them away from each other. The structures discussed in this study are those which are formed when the net force on each charge is zero.

2.1. Finding The Structures

When multiple charged particles are placed in an electric field, they experience a force due to the Coulomb interaction between them. This force is directly proportional to the product of the charges and inversely proportional to the square of the distance between them. Thus, if two particles have the same polarity, they will repel each other.
In addition to the Coulomb interaction, the particles in this system are also subject to a harmonic potential that confines them to two dimensions. This potential is analogous to a spring, in that it exerts a force on the particles that is proportional to the origin.
The equilibrium positions of the particles are those at which the net force on each particle is zero. In other words, the forces due to the Coulomb interaction and the harmonic potential balance each other out, so the particles remain in a stationary configuration. These equilibrium positions correspond to the structures that are analysed in this study.
The total energy $\tilde{E}$ of a cluster of N charges Q, confined by a 2D isotropic harmonic potential, is found by adding the confinement potential and the coulomb repelling energy:

$$\tilde{E} = \frac{1}{2}\sum_{i}^{N}(k_x X_i^2 + k_y Y_i^2) + \frac{Q^2}{4\pi\epsilon_0}\sum_{i<j}^{N}[(X_i - X_j)^2 + (Y_i - Y_j)^2]^{-1/2} \tag{2.1}$$

where X_i and Y_i are the Cartesian coordinates of the i$^t h$ charge, while k_x and k_y are the force constants for the confining potential in the x and y directions.

For convenience, this has been non-dimensionalised, i.e. manipulated such that it no longer needs units. This means $a = \frac{Q^2}{4\pi\epsilon_0}$ and $E = \tilde{E}/(a^{2/3}(k_x + k_y)^{1/3})$ are used which yields the equation:

$$E = \frac{1}{2}\sum_{i}^{N}(x_i^2 + y_i^2) + \sum_{i<j}^{N}[(x_i - x_j)^2 + (y_i - y_j)^2]^{-1/2} \tag{2.2}$$

where $x_i = X_i/l_0$ and $y_i = Y_i/l_0$ are dimensionless coordinates for $l_0 = (a/k)^{1/3}$.

The dimensionless energy E is calculated through solving Equation (2.2), how the coordinates of the points of each structure are found is explained in Section 3. A sample of the resulting plots can be seen in Fig. 2.1.

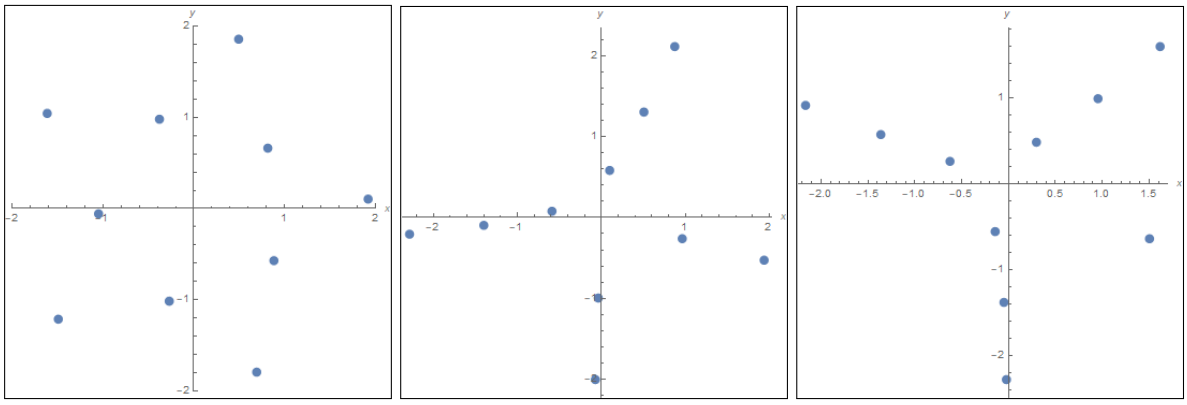

(a) E = 35.958 (b) E = 37.851 (c) E = 38.429

Figure 2.1.: Example of three equilibrium structures, for various energies, E. Points represent position of ions.

2.2. Stable and Unstable Equilibrium

In a 'stable' equilibrium, a system will return to its original location if it is displaced [6]. In other words, if you push the system away from its equilibrium position, it will tend to return to that position on its own. An example of stable equilibrium is a pendulum hanging vertically because if it is moved slightly, it will swing back and forth until it comes to a halt in its original position.
In contrast, a system that is in a state of 'unstable' equilibrium will not return to the original location if displaced but instead passes into a new state of stable equilibrium [6]. An example of unstable equilibrium is an inverted pendulum because if it is nudged even slightly, it will fall over.
In terms of these ion configurations, a structure in stable equilibrium will return to its original configuration if the ions are perturbed. Any structure that does not do this is considered unstable.

2.3. Voronoi Entropy

Voronoi entropy is a mathematical technique for measuring the symmetry of points - or seeds - scattered across a surface [7]. There is an area, known as a Voronoi cell, site, or generator, for each seed that is made up of all points in the plane that are closer to that seed than to any other point. The Voronoi polyhedron of a point in space is the smallest polyhedron formed by the perpendicularly bisecting planes between a given seed and all the other seeds [8]. Voronoi diagrams divide a region into space-filling, nonoverlapping convex polyhedra, as shown in Fig. 2.2.
The Voronoi entropy is a measure of the orderliness or uniformity of the Voronoi diagrams, and is given by the formula:

$$S = -\sum_{n=3} P_n ln P_n \tag{2.3}$$

where P_n is the fraction of polygons with n sides or edges in a given Voronoi diagram [7, 8] . So if there are 10 polygons in a Voronoi diagram and 3 of them have n number of sides, then $P_n = \frac{3}{10}$.

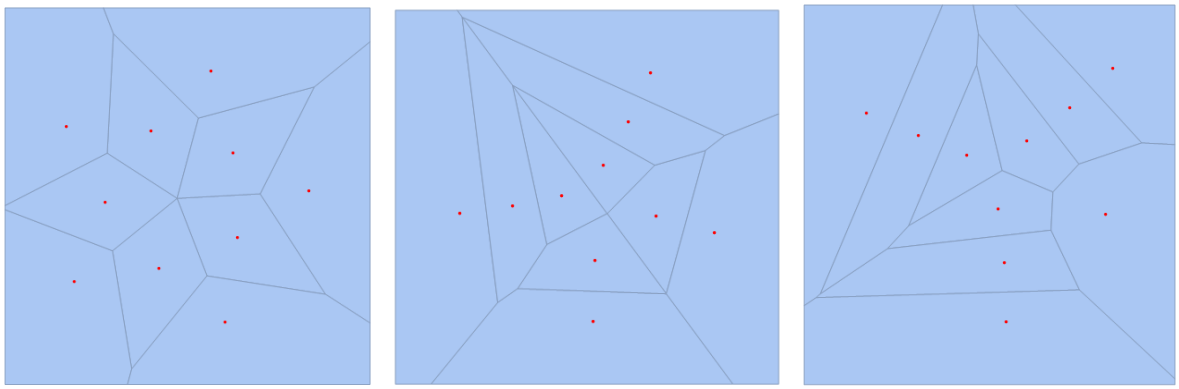

(a) E = 35.958, S = 1.05 (b) E = 37.851, S = 1.33 (c) E = 38.429, S = 1.42

Figure 2.2.: Example of the Voronoi diagram of three equilibrium structures, for various energies, E. Points represent position of ions.

The summation in Equation (2.3) is performed from n=3 to the maximum number of sides of any polygon in the Voronoi diagram. The Voronoi entropy provides a way to quantify the complexity of a point distribution, i.e. the degree of irregularity or diversity of the points in a pattern. In the case where all the polygons have the same number of sides, $P_n = 1$. This occurs when points are arranged in a perfectly uniform pattern, resulting in identical cells around each seed. Thus the Voronoi entropy becomes zero for a perfectly ordered structure, consisting of a single type of polygon. Therefore, it is expected that for a more symmetrical structure, the value of S decreases, whereas an irregular distribution of points will have a higher value of S [7].
The outer boundary of the diagram is known as a bounding box. In practice, a rectangular bounding box is often used for Voronoi diagrams, out of convenience, as it is a simple and familiar shape, and it is easy to define the distance metric in a rectangular coordinate system. However, in principle, Voronoi diagrams can be defined for points in any shape with a well-defined distance metric [9]. It is important to note that the Voronoi entropy is not an absolute measure of complexity, but rather a relative measure that depends on the choice of boundary box as well as the distribution of the input points within that box. Therefore, different choices of boundary box can result in different Voronoi entropy values for the same set of input points.

2.4. Radial Distribution Function

The Radial Distribution Function (RDF) describes the probability density of finding particles at a certain distance from a reference particle in a system of particles [10]. It is calculated by counting the number of particle neighbours as a function of distance, r, with respect to a reference particle and taking the ensemble average [10]. Mathematically, this is given as:

$$g(r) = \frac{1}{\rho N} \sum_{i \neq j}^{N} \delta(r - r_{ij}) \tag{2.4}$$

where $g(r)$ is referred to as the radial distribution function, ρ is the number density of the system, N is the total number of particles in the system, δ is the Dirac delta function, and r_{ij} is the distance between particles i and j. For the purposes of this work, $N = 10$. The sum $\sum_{i \neq j}^{N}$ is taken over all pairs of particles in the system, excluding the case where i=j (i.e. the

distance between a particle and itself). The term $\delta(r - r_{ij})$ represents a "spike" at the distance r_{ij}. It is equal to 1 if r is exactly equal to r_{ij}, and 0 otherwise. This term is used to count the number of pairs of particles that have a distance r from each other. The factor $\frac{1}{\rho N}$ normalises the RDF which ensures that the RDF provides a relative measure of the probability of finding particles at different distances, rather than an absolute measure, such that:

$$\int_0^\infty g(r)dr = 1 \tag{2.5}$$

In summary, the RDF tells us how particles are distributed relative to each other in a system.

2.5. Gestalt Theory

Gestalt theory is a psychological approach that emphasises the importance of understanding the whole rather than just the individual parts. While the positions of points, the locations of the ions, are found through numerical solutions to an electrostatics problem (see Section 3), Gestalt theory says that our brains organise these points into patterns based on how they relate to each other [11]. In our case, we mostly focus on the laws of proximity and continuation. The law of proximity states that when an individual perceives an assortment of objects, they perceive objects that are close to each other as forming a group [11]. The law of continuity, on the other hand, says that elements of objects tend to be grouped together, and therefore integrated into perceptual wholes if they are aligned within an object [11].
This is why the human brain interprets these structures as patterns, despite the points in these configurations being randomly distributed.

3. Computational Method

Wolfram Mathematica was used for all the computations in this work. Once this had produced data, spreadsheets were generated in order to compare and contrast the results. The stable structures were found in a slightly different way to the unstable ones.

3.1. Stable Equilibrium

Stable equilibrium states may be obtained by direct minimisation of energy (Equation. 2.2). For 10 charges, 50 random initial configurations were generated and their respective energies minimised, using the method of Gradient Descent. Gradient Descent is a first-order iterative optimisation algorithm. The theory is to take repeated steps in the opposite direction of the gradient at a given point. This gradient tells us the direction of steepest descent, so the parameters are updated to move that direction. [12, 13]. For a small number of ions, systems typically possess only a few stable minima. Therefore, 50 iterations is sufficient to be confident that all of the stable minima have been identified [1].

3.2. Unstable Equilibrium

In order for Equation (2.2) to produce a stationary solution, it is necessary that:

$$\frac{\partial f}{\partial x_i} = 0 \quad and \quad \frac{\partial f}{\partial y_i} = 0 \qquad for\, i = 1, ..., N. \tag{3.1}$$

So in order to obtain a function that satisfies both of these properties, we square both $\frac{\partial f}{\partial x_i}$ and $\frac{\partial f}{\partial y_i}$, add them together, and then sum up to N:

$$f = \sum_{i}^{N} \left(\left(\frac{\partial f}{\partial x_i} \right)^2 + \left(\frac{\partial f}{\partial y_i} \right)^2 \right) \tag{3.2}$$

The program then looks to minimise this f and search for the cases in which it vanishes. Again, this is done via Gradient Descent, as well as the Newton-Raphson Method.
The algorithm that was employed to find these solutions begins with a randomised starting configuration of points in the x-y plane and then seeks to minimise f numerically, with respect to these coordinates. If f is below a certain tolerance (1 x 10^{-10}), then that state is taken to be in equilibrium [1]. See Appendix A for more detail on the Newton-Raphson Method.

3.3. Structure Analysis

With the coordinates of the points of each structure found, as explained above, Mathematica was used to create a list plot of each structure.

Each point in one of these plots was connected to its nearest neighbour. This was done by paring each ion to the next closest one to it and joining them using a straight line, as seen in Fig. 3.1. These graphs are referred to in this work as "Nearest Neighbour Graphs" or "Nearest Neighbour Diagrams." Then the Euclidean distances of all these lines were measured and divided by the total number of lines. These means, which were found for each structure, gave what is called the "Average Nearest Neighbour Distance," which is discussed later.

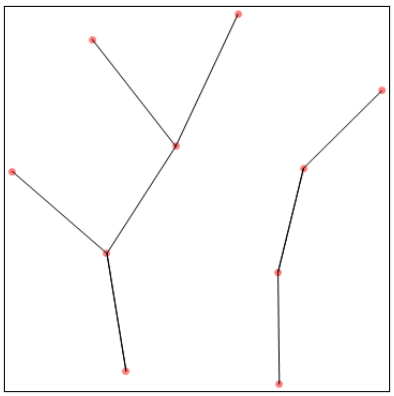

Figure 3.1.: Example of a nearest neighbour diagram of a structure of 10 ions

Mathematica's Voronoi Diagrams tool was used to create images like the ones in Fig. 2.2. Once, these diagrams were generated, Mathematica could be utilised to find the Voronoi Entropy by counting the number of sides in each polygon and computing S from Equation (2.3).
To find the Radial Distribution Function, first the Euclidean distances between all the points in a structure is measured using the "DistanceMatrix" tool. Then these distances are sorted into bins and a histogram is made to show how frequently distances within a certain range occur. Then each distance is divided by the average of its bin of the histogram. The "BinCounts" function is used to count the number of distances in each bin. Then g(r) is plotted in a plot against r, using Equation (4). This graph demonstrates the relative probability of finding a point at a given distance from another point. An example of the Radial Distribution Function for 10 points in a straight line can be seen in Fig. 3.2.

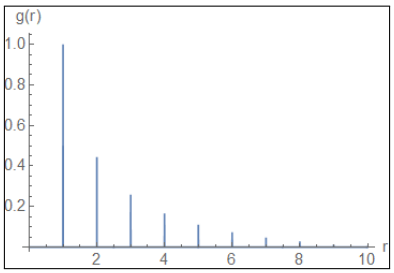

Figure 3.2.: Radial Distribution Function for a straight line of 10 points.

This "DistanceMatrix" tool was also employed to find both the average distance between all the points in a structure and the average distance between each point in a structure and the origin.

4. Results

4.1. Unstable Structures

Using the method described in Section 3.2, a total of 970 structures in unstable equilibrium were found.
For higher energies, there was bigger gaps between energy values and more structures with the same energy. Fig. 4.1 shows that multiple solutions have the same energies which suggests some identical arrangements, as in Fig. 4.2.

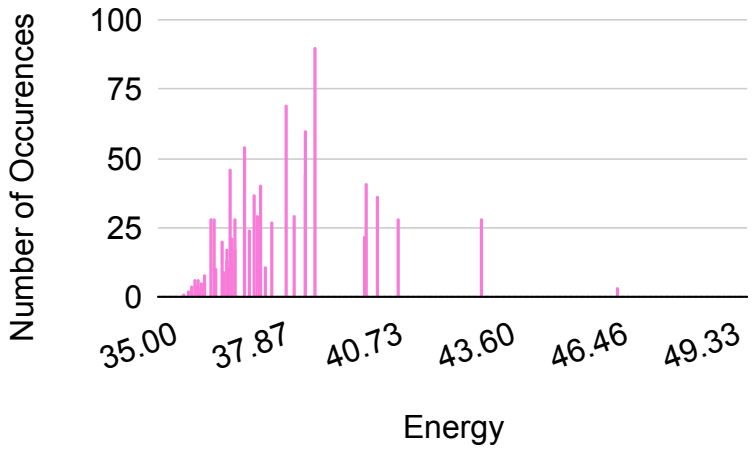

Figure 4.1.: Histogram displaying the number of configurations against energy, for bin width 0.01

In order to find the number of unique structures, the nearest neighbour distances and energies for each structure were analysed and if they were all the same for multiple structures, the duplicate or identical patterns were ignored. Each energy had its own unique arrangement, there were no two different structures which shared an energy up to an energy precision of 10^{-6}. Out of the total of 970 structures, 53 distinct arrangements were found.
This means there are 53 different configurations where the net force on each ion is zero. However, it is possible that if the program were to be ran more times, more structures could be found, since some structures were much more likely to appear than others. For example the pattern found in Fig. 4.3 was found 90 times, whereas there were 5 structures which only appeared once, as seen in Fig. 4.4.

4.1.1. Likelihood of a Structure Being Found

Visually, there is nothing strikingly different about the structures that appeared most frequently, as opposed to least frequently.

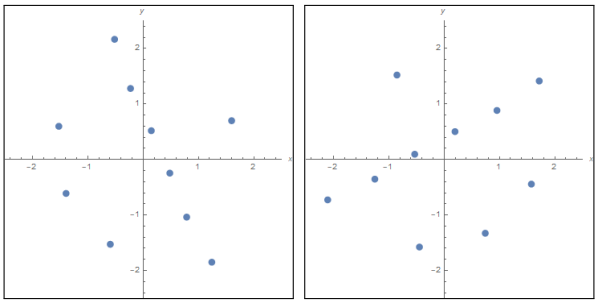

Figure 4.2.: Example of two identical structures, each with E = 36.938182.

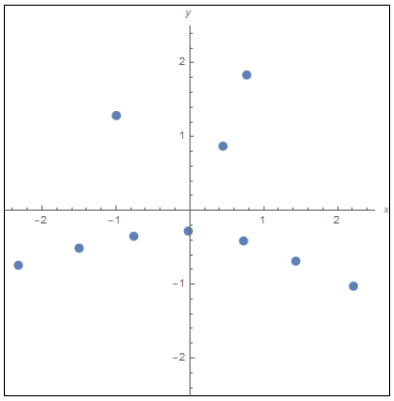

Figure 4.3.: Most frequently occurring equilibrium pattern, 90 occurrences, with E = 38.971416.

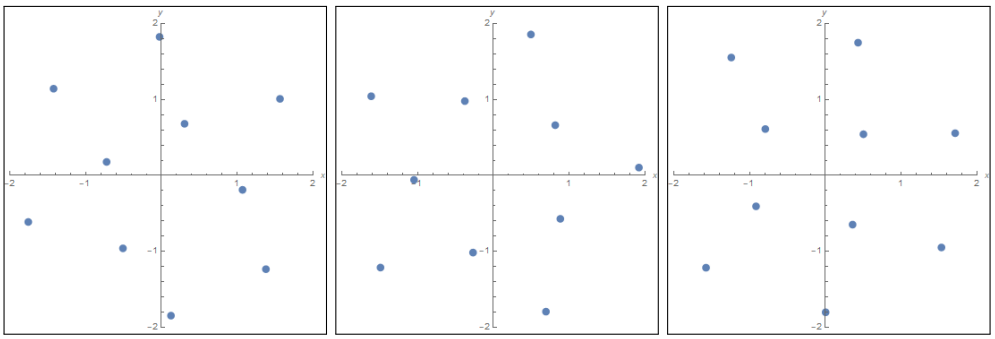

(a) E = 35.851144 (b) E = 35.957548 (c) E = 35.963059

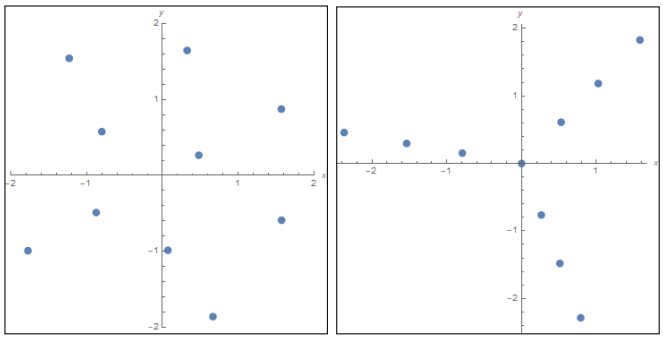

(d) E = 36.042905 (e) E = 40.264993

Figure 4.4.: Equilibrium patterns which were found only once

Investigation of the graph showing number of occurrences as a function of energy, Fig. 4.5 implied that there could be some relationship between these two variables. At lower energies fewer samples were found. More were found for high energy, with a peak when the energy was E = 38.971416. However, as energy increased beyond that value, the number of occurrences began to fall again. This resulted in a correlation coefficient of 0.34 which is not indicative of a strong relationship. However, it would be interesting to produce this graph for more ions to see if these changes would result in a higher correlation. It is possible that the relatively small number of ions resulted in a weaker relationship.

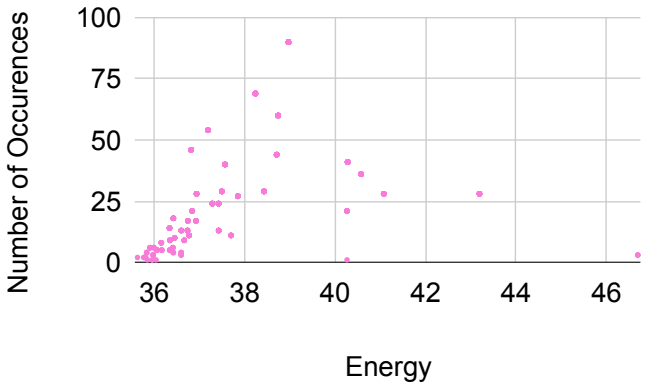

Figure 4.5.: Scatter plot showing number of occurrences as a function of energy.

The correlation coefficient between the Mean Nearest Neighbour Distance and the Number of Occurrences, shown in Fig. 4.6, was similar at -0.33. This can be explained by the high negative correlation between Average Nearest Neighbour Distance and Energy, as discussed in the next section.

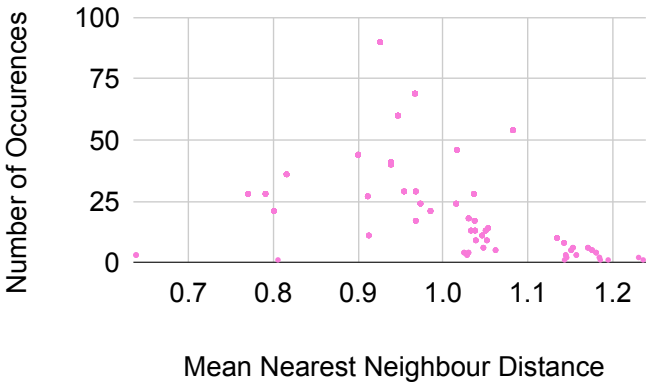

Figure 4.6.: Scatter plot showing number of occurrences as a function of nearest neighbour distance.

4.1.2. Nearest Neighbour Distance

The distance of each point in a structure to its nearest neighbouring point was calculated and then divided by the total number of points in order to find the average distance between nearest neighbours. The range of average nearest neighbour distances was from d = 0.637961,

for energy E = 46.691684 (Fig. 4.7a), and d = 1.23596, for energy E = 35.957548 (Fig. 4.7b).

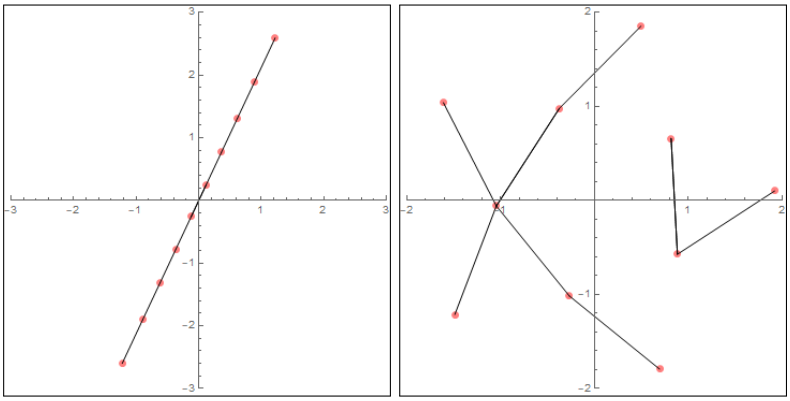

(a) d = 0.64, E = 46.7 (b) d = 1.2, E = 35.96

Figure 4.7.: The structures which had the highest and lowest average nearest neighbour distance.

It was found that as the energy of structures increased, the charges became closer to the next charge. The correlation coefficient between these two variables was found to be -0.87. The relationship between these variables is demonstrated in Fig. 4.8.

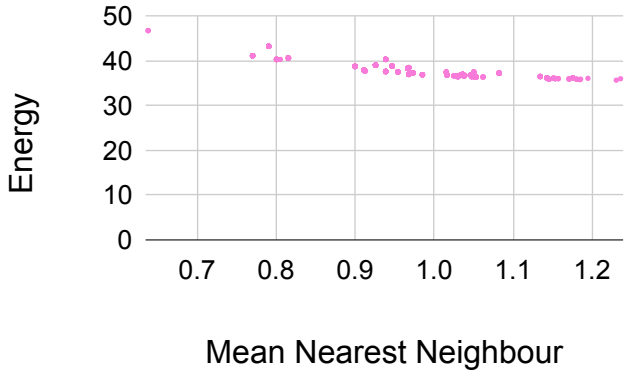

Figure 4.8.: Scatter Plot showing the Relationship between Energy and Mean Nearest Neighbour Distances

4.1.3. Voronoi Entropy

The range of Voronoi entropies found for the different structures was from S = 0, the most symmetric, which had E = 46.691684 (Fig. 4.9), to S = 1.60944, the least, symmetric which had E = 36.737621 (Fig. 4.10).
Although the most symmetric structure was that with the highest energy. The opposite was not true. The structure with the lowest energy, E = 35.632424, had a Voronoi Entropy of S = 1.0889, which is neither high nor low, when compared to all the values of S for unstable structures. Additionally, the structure with the highest Voronoi entropy did not have a particularly low energy. Furthermore, the graph of the relationship, as shown in Fig. 4.12, does not suggest a

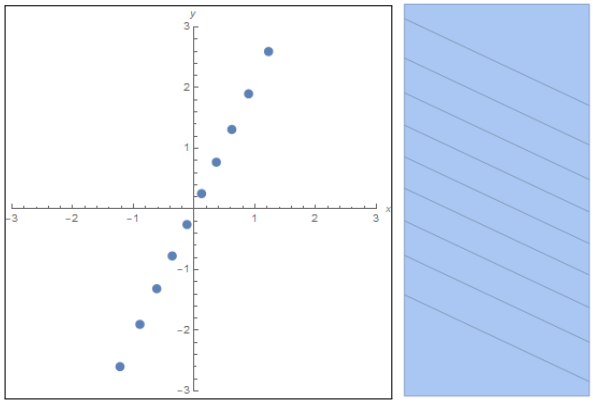

(a) (b)

Figure 4.9.: The most symmetric structure, having energy E = 46.691684 and Voronoi Entropy of S = 0

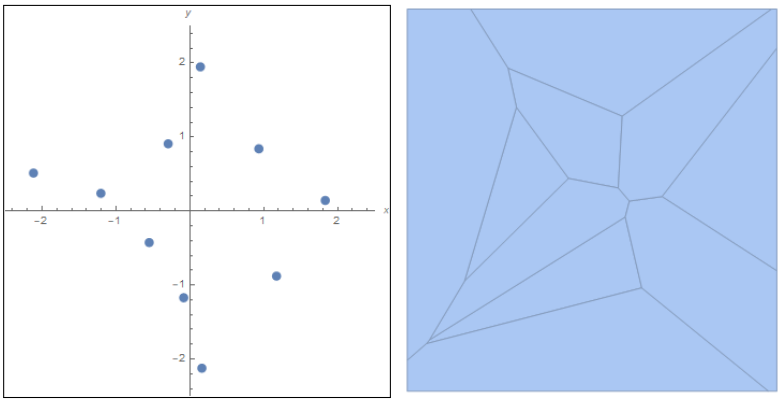

(a) (b)

Figure 4.10.: The least symmetric structure, having energy 36.737621 and Voronoi Entropy of S = 1.60944

correlation, nor does the correlation coefficient of -0.149. Similarly, the correlation coefficient for the graph of Voronoi entropy and average nearest neighbour distance was 0.056. Therefore, we cannot conclude that Voronoi entropy has any dependence on either of these variables.
The correlation coefficient between number of occurrences and Voronoi Entropy was slightly higher, at 0.41 but still not statistically significant.The graph might suggest the possibility of an inter-dependency, with the most common arrangements having relatively high Voronoi arrangements, but this is not sufficient to show a correlation. This relationship is demonstrated in Fig. 4.11.
The scatter plot, Fig. 4.12, demonstrates that there are a lot of configurations with Voronoi entropy around the value of 1. This indicates a high degree of disorder and a lack of symmetry in the arrangement of particles. In other words, the Voronoi diagram of the system is highly irregular, with large fluctuations in the sizes and shapes of the Voronoi cells. This suggests that the particles are distributed randomly, without any preferred arrangement or structure.

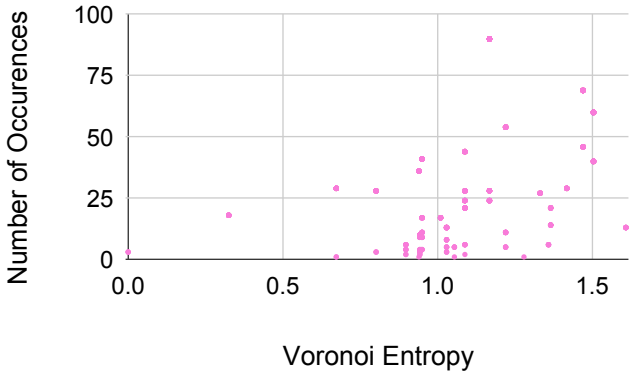

Figure 4.11.: Scatter Plot Showing Number of Occurrences as a Function of Voronoi Entropy.

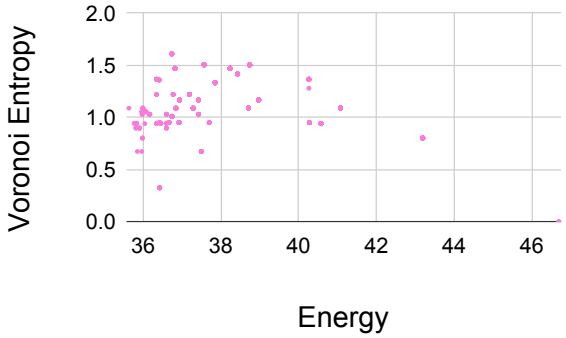

Figure 4.12.: Scatter Plot showing the Relationship between Voronoi Entropy and Energy.

4.1.4. Radial Distribution Function

Radial Distribution Function (RDF) graphs were used to show the probability of finding an ion at a certain distance away from another ion in the structure. A higher value of g(r) indicates a greater likelihood of finding an ion at that distance. Peaks in the graph represent distances where many ions are found, while smaller values indicate distances where fewer ions are found. For instance, Fig. 4.13 demonstrates the RDF graph for the structure with the lowest energy, E = 35.632424. Here we see g(r) starts at r = 1.18 at a value g(r) $\approx$ 0.6, it then begins to reduce slightly before a big peak at r = 1.35, indicating that there were many ions at that distance. After that it reduces fairly slowly, except for another, smaller peak at r = 2.16.

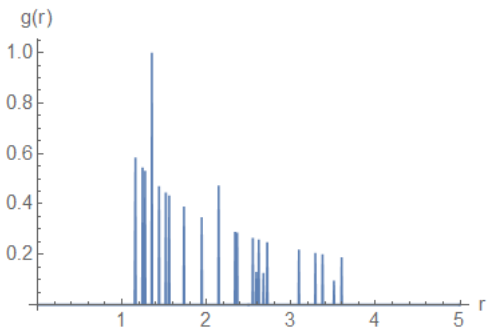

Figure 4.13.: Radial Distribution Function for the structure with the lowest energy.

On the other hand, the Radial Distribution Function for the structure with the highest energy, E = 46.691684, can be seen in Fig. 4.14, as mentioned in section 4.1.3, this was also the structure with lowest Voronoi entropy, S = 0. As can be expected from its pattern, out of all the configurations its RDF graph most closely resembles that of 10 points in a straight line, equidistant from each other (Fig. 3.2), indicating that the distances between the ions were the most regular compared to all the other structures. However, the decrease in g(r) is not as consistent as that of a line, indicating some slight variations in the distances between ions. This means that not all points were exactly the same distance away from their nearest neighbour but the distances between an ion and every other ion was still the most regular out of those presented.

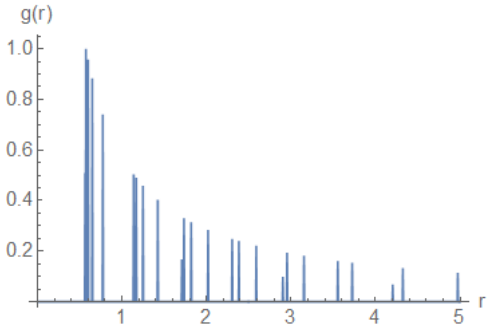

Figure 4.14.: Radial Distribution Function for the structure with the highest energy.

Finally, the graph of the RDF with the highest Voronoi is represented by Fig. 4.15 . This begins at r = 0.9, with a high value of g(r). It then decreases in a relatively similar fashion to Fig. 4.14, except for two peaks at r = 2.44 and r = 3.05.

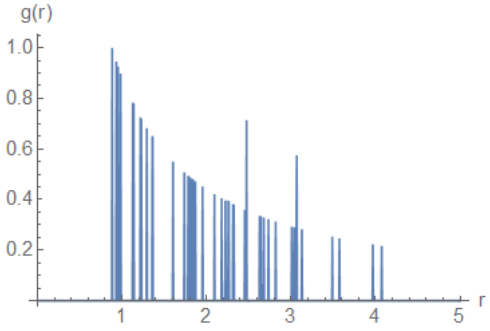

Figure 4.15.: Radial Distribution Function for the structure with the highest Vornoi entropy.

The mean distance between points in a structure, $\bar{r}$, ranged from $\bar{r} = 2.1628$, for E = 35.63, to $\bar{r} = 2.25036$, for E = 46.69. So the configuration with the smallest $\bar{r}$, also had the lowest energy and the configuration with the largest $\bar{r}$, also had the highest energy. Furthermore, having a correlation coefficient of 0.97, $\bar{r}$, is almost perfectly correlated with energy (which would make sense from Equation 2.2). This relationship is shown in Fig. 4.16.Therefore, for higher energies, points closer to their nearest neighbour, but they are farther away from every other point in the system. The correlation coefficients between this and the other variables studied are visible below, in Table 4.1, which summarises the results.
The mean distance of points from origin, $\bar{d}_0$, had very little fluctuation with respect to energy, indicating that, on average, points are always roughly the same distance away from (0,0),

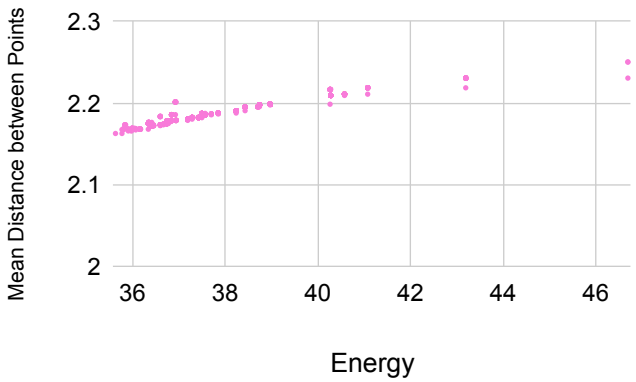

Figure 4.16.: Scatter plot showing the relationship between mean distance between points and energy.

regardless of structure. The minimum, $\bar{d}_0 = 1.43051$, occurred for E = 38.74 and the maximum, $\bar{d}_0 = 1.5689$, occurred for E = 36.93. This lack of dependence on energy is also evident from the graph of energy against this distance, Fig. 4.17, which had a correlation of -0.2. The correlation coefficients between this and the other variables studied are visible below, in Table 4.1, which summarises the results.

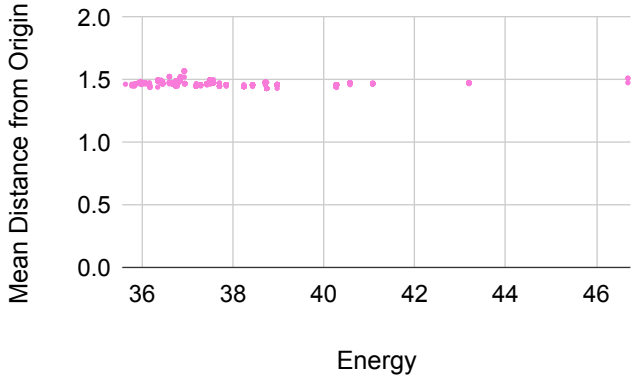

Figure 4.17.: Scatter plot showing the relationship between mean distance of points from origin and energy.

	E	d	S	Occ	$\bar{r}$	d_0
Max	46.69	1.24	1.61	90	2.25	1.57
Min	35.63	0.64	0	1	2.16	1.43
E		-0.87	-0.14	0.34	0.97	-0.2
d	-0.87		0.056	0.33	-0.9	0.03
S	-0.14	0.056		0.41	-0.11	-0.38
Occ	0.34	-0.33	0.41		0.32	-0.4
$\bar{r}$	0.97	-0.9	-0.11	0.32		-0.07
d_0	-0.2	0.03	-0.38	-0.4	-0.07	

Table 4.1.: A table summary of the results for the unstable structures, showing the max and min of each variable and its correlation coefficient with the other variables.

4.2. Stable Structures

A total of two stable structures were found, using the method detailed in Section 3.1. Their energies were found to be 35.51952007 (Fig. 4.18a) and 35.62257055 (Fig. 4.18b). This is lower than any of the unstable equilibriums. The lower of these, E = 35.51952007, is very close to or is actually the absolute ground state of the system, since the lowest energy state represents a state of equilibrium where the system is stable [14]. The energy of a structure is calculated by finding a balance between the attractive forces that bring ions closer together and the repulsive forces that push them farther apart. In the case of the stable structures, this balance is such that the ions are able to maintain a more regular and stable arrangement at a lower energy than the unstable arrangements.

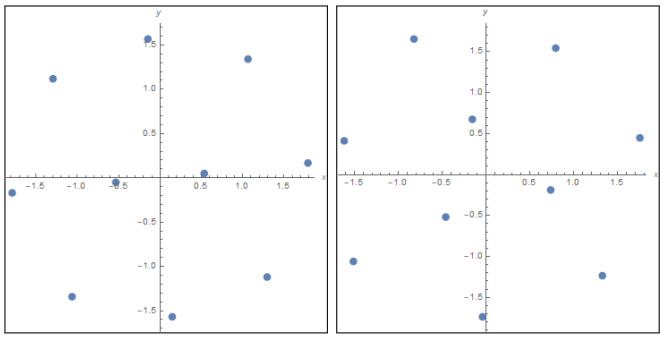

(a) E = 35.51952007 (b) E = 35.62257055

Figure 4.18.: The two stable structures that were found.

These energies corresponded to fairly large mean nearest neighbour distances, 1.21826 and 1.26043, respectively. This is significant as the largest average for the stable structures was 1.23596, further demonstrating the relationship between energy and this nearest neighbour distance. The nearest neighbour graphs of these structures is demonstrated in Fig. 4.19.
The Voronoi diagrams of these stable structures are displayed in Fig. 4.20. Their Voronoi Entropy was found to be 0.950271 and 0.801819, respectively. This implies a fair amount of disorder, but still both values of S were less than 1. This is unlike the unstable structures which had many values where S was greater than 1.
The radial distribution functions for the two stable structures are displayed in Fig. 4.21. The

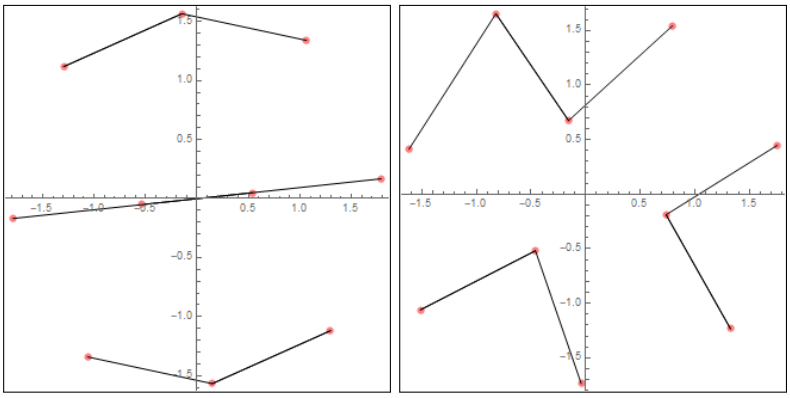

(a) E = 35.51952007 (b) E = 35.62257055

Figure 4.19.: The nearest neighbour graphs for the two stable structures.

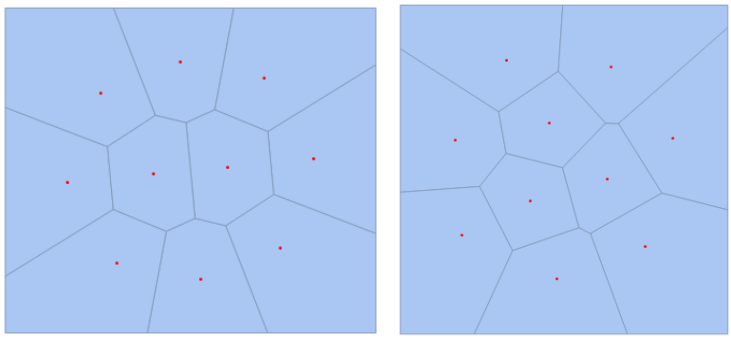

(a) E = 35.5, S = 0.95 (b) E = 35.6, S = 0.80

Figure 4.20.: The Voronoi diagrams of the two stable structures that were found.

pattern with energy E = 35.51952 starts off with a relatively small g(r), then peaks at around r = 1.2 and then decreases uniformly as r increases. The pattern with energy E = 35.62257 has a large initial g(r), and then reduces as r gets bigger, except for around r = 2.4, where there is another peak.

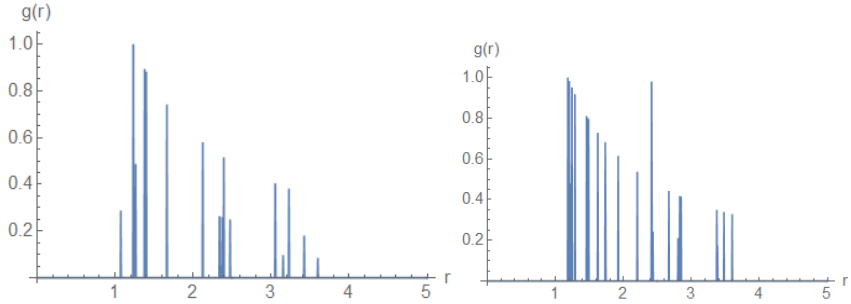

(a) E = 35.51952 (b) E = 35.62257

Figure 4.21.: The Radial Distribution Function of the two stable structures that were found.

The mean distance between points in the stable structures was similar to that of the unstable structure with the lowest energy, with $\bar{r} = 2.16423$ and $\bar{r} = 2.16181$, respectively. The mean

distance of points from the origin were $\bar{d}_0 = 1.46697$ and $\bar{d}_0 = 1.46072$, respectively.

	Stable 1	Stable 2
E	35.52	35.62
d	1.22	1.26
S	0.95	0.80
$\bar{r}$	2.16	2.16
$\bar{d}_0$	1.47	1.46

Table 4.2.: A table summary of the results for the stable structures, showing the values of all quantifiable variables studied.

5. Visual Aspects

The structures described in this work are point configurations, arranged in such a way as to suggest the existence of lines, arcs, and isolated points. The simplest way to compute lines between points is using a Nearest Neighbour graph, as described in Section 3.3.

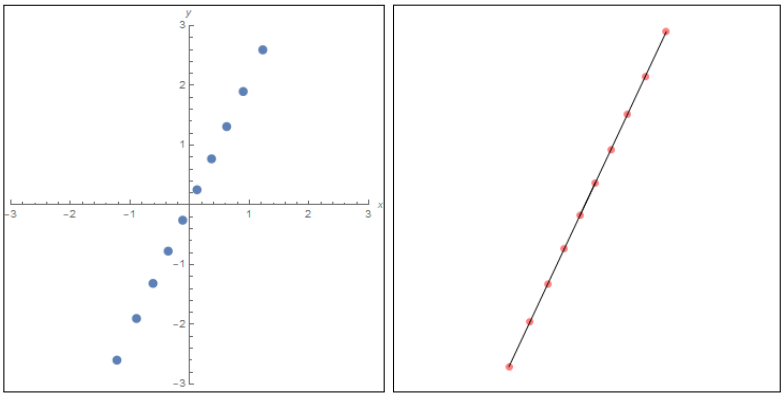

(a) E = 46.69 (b) Nearest Neighbours Graph

Figure 5.1.: A sample equilibrium state and its respective Nearest Neighbour Graph

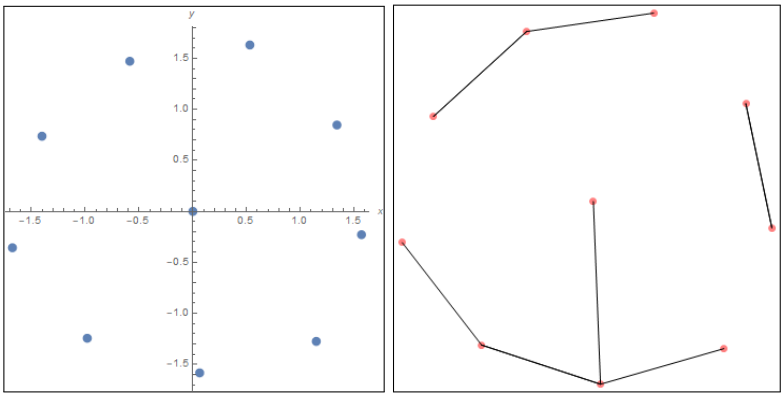

(a) E = 35.83 (b) Nearest Neighbours Graph

Figure 5.2.: A sample equilibrium state and its respective Nearest Neighbour Graph

Some of the connections made by the program are in line with what we would expect, for example in Fig. 5.1, the points that are joined using this nearest neighbour method are in line with the connections the brain would make but that was not always the case. The connections made in Fig. 5.1b by this program are not what we would expect to be linked from just looking at the points in Fig. 5.1a.

6. Outlook

These findings provide valuable insights into the behaviour of Coulomb crystals in 2D, with potential applications in fields such as quantum computing. However, further research is needed to fully understand the relationships between variables and the significance of these findings for practical applications.
As suggested previously, the methods that were applied in this work could be repurposed for similar systems but with more ions. This work used a system of 10 ions due to a trade-off between configuration size and computational feasibility. However, a greater number of charges may lead to stronger relationships than the ones seen here.
During this study, it was noted that there was not a huge fluctuation in energy, with a range from E = 35.52 to E = 46.69 The reason for this and the implications it has are a possible avenue for future research.
One could also approach Voronoi entropy from another angle. As briefly mentioned in Section 2.3, the Voronoi entropy depends not only on the configuration of points but also the bounding box. Therefore, an analysis of Voronoi entropy for different bounding boxes could lead to different results. The results of multiple processes, for a variety boundaries, could be analysed and compared in order to determine if both methods find the same conclusion or if there's a discrepancy in how symmetric a given pattern is, for different bounding boxes.
Instead of the electric potential which was discussed here, i.e. a Penning trap, the same analyses could be performed for a magnetic potential, i.e. a Paul trap, and the results compared with those found in this study.
Section 5 highlights the limitations with joining up points, only using nearest neighbours. More effort can be put into finding new ways to connect these points in a way that is more intuitive, perhaps using splines instead of straight lines. Alternatively, telling the program to take the path of least change i.e. maximising the dot product between one point and the next.
Another novel idea would be to see what applications this research has outside of the realm of physics. These structures resemble some pieces of computer generated art and could play a role in this ever growing field. Additionally, the way the lines are connected using the nearest neighbour method are not always the same as those perceived by the human brain when looking at them. Thus, one could examine the differences and similarities between how a group of people connect the dots versus what a computer links together.

7. Conclusion

In this study, we analysed, via computer simulation, a variety of equilibrium states for 2D Coulomb crystals with 10 ions, using energy as well as techniques such as nearest neighbour distances, Voronoi entropy, and radial distribution functions. A wide variety of stationary states were found.

Out of the 970 unstable structures, 53 unique patterns were found. There seemed to be a correlation between the energy of a structure and how frequently it occurred, with the most commonly found structure having an energy of E = 38.971416.

With increasing energy, the average nearest neighbour distance of a structure decreased, meaning the ions are closer to the next ion. This relationship had a significant correlation coefficient of -0.87. The energies ranged from E = 35.632424 and E = 46.691684. The average nearest neighbour distances were between d = 0.637961 and d = 1.23596. However the average distance between all the ions in a structure increased for higher energies. This distance ranged from $\bar{r}$ = 2.16 to $\bar{r}$ = 2.25 and had a correlation coefficient with energy of 0.97. So even though, for higher energies, neighbouring ions were closer together, the ions, on average, were further away from each other.

Symmetry of structures was measured using Voronoi entropy. A variety of values of Voronoi entropy were found for the unstable configurations, ranging from S = 0 to S = 1.60944, with a possible but ultimately inconclusive relationship with energy and number of occurrences.

The radial distribution functions of a selection of the configurations were investigated and compared against each other and against the RDF of 10 points in a straight line. It was found that the most regular RDF of any configuration was that of the structure with the highest energy and lowest Voronoi entropy, indicating that the distances between the ions in this structure was the most consistent.

The two stable structures had lower energies than any of the identified unstable ones. This corresponded to a higher average nearest neighbour distance for most of if not all the unstable arrangements. The two stable structures had Voronoi entropies of S = 0.950271 and S = 0.801819. The RDF of the structure with energy E = 35.51952 was incredibly irregular, whereas that for the structure with E = 35.62257 more closely resembled the others and that of the straight line.

Regardless of the structure, the average distance of points from the origin remained almost constant in relation to energy, indicating minimal fluctuations, meaning that the points tend to be at approximately the same distance from (0,0).

Ultimately, this study provides important insights into the complex behaviour of 2D Coulomb crystals, and offers a foundation for further research that could lead to practical applications in fields such as quantum computing, computer-generated art, psychology, and beyond.

Bibliography

[1] Mughal, A., S. Hutzler, and D. Weaire. "Equilibrium states of confined ions in two dimensions." *Philosophical Magazine* (2023): 1-15.

[2] Mughal, A., S. Hutzler, and D. Weaire. "Coulomb Calligraphy." *Unpublished*.

[3] Landa, H., Reznik, B., Brox, J., Mielenz, M., and Schätz, T. "Structure, dynamics and bifurcations of discrete solitons in trapped ion crystals." *New Journal of Physics* 15.9 (2013): 093003.

[4] Cirac, Juan I., and Peter Zoller. "Quantum computations with cold trapped ions." *Physical Review Letters* 74.20 (1995): 4091.

[5] Porras, Diego, and J. Ignacio Cirac. "Quantum manipulation of trapped ions in two dimensional Coulomb crystals." *Physical Review Letters* 96.25 (2006): 250501.

[6] Hay, James. *The biomechanics of sports techniques.* Prentice-Hall, 1978.

[7] Bormashenko, Edward, Frenkel, M., Vilk, A., Legchenkova, I., Fedorets, A.A., Aktaev, N.E., Dombrovsky, L.A. and Nosonovsky, M. "Characterization of self-assembled 2D patterns with Voronoi Entropy." *Entropy* 20.12 (2018): 956.

[8] Senthil Kumar, V., and V. Kumaran. "Voronoi cell volume distribution and configurational entropy of hard-spheres." *The Journal of Chemical Physics* 123.11 (2005): 114501.

[9] Kim, Deok-Soo, Donguk Kim, and Kokichi Sugihara. "Voronoi diagram of a circle set from Voronoi diagram of a point set: II. Geometry." *Computer Aided Geometric Design* 18.6 (2001): 563-585.

[10] Sha, Wei, Xiaomin Wu, and Kim Ghee Keong. *Electroless copper and nickel-phosphorus plating: processing, characterisation and modelling.* Elsevier, 2011. Shanks, Brennon L., Jeffrey J. Potoff, and Michael P. Hoepfner. "Transferable Force Fields from Experimental Scattering Data with Machine Learning Assisted Structure Refinement." *The Journal of Physical Chemistry Letters* 13.49 (2022): 11512-11520.

[11] Stevenson, Herb. "Emergence: The gestalt approach to change." *Unleashing executive and orzanizational potential*. Retrieved 7 (2012).

[12] Fletcher, Reeves, and Colin M. Reeves. "Function minimization by conjugate gradients." *The Computer Journal* 7.2 (1964): 149-154.

[13] Haji, Saad Hikmat, and Adnan Mohsin Abdulazeez. "Comparison of optimization techniques based on gradient descent algorithm: A review." *PalArch's Journal of Archaeology of Egypt/Egyptology* 18.4 (2021): 2715-2743.

[14] Pickard, Chris J., and R. J. Needs."Ab initio random structure searching." *Journal of Physics: Condensed Matter* 23.5 (2011): 053201.

[15] Akram, Saba, and Quarrat Ul Ann. "Newton raphson method." *International Journal of Scientific & Engineering Research* 6.7 (2015): 1748-1752.

A. Appendix A

Newton-Raphson Method

The Newton–Raphson method is an approach of finding approximations to the roots of a function [15]. It is based on the Taylor Expansion of a function, f, about a given point, a:

$$f(a+h) = f(a) + hf'(a) + h^2 f''(a) + ... \tag{A.1}$$

For matters of simplicity, the series can be truncated at the linear term in h to approximate the function:

$$f(a+h) = f(a) + hf'(a) + \mathcal{O}(h^2) \tag{A.2}$$

Then setting $f(a+h) = 0$ and solving for for h:

$$h = -\frac{f(a)}{f'(a)} \tag{A.3}$$

Thus, given an approximation for a root, x_n, a more accurate approximation, x_{n+1}, can be determined by the formula below:

$$x_{n+1} = x_n - \frac{f(x_n)}{f'(x_n)} \tag{A.4}$$

B. Appendix B

The 2 stable structures that were found by the program detailed in Section 3.1 and subsequently analysed for the purposes of this work, they are arranged by energy, in increasing order, from E = 35.51952 to E = 35.62257.

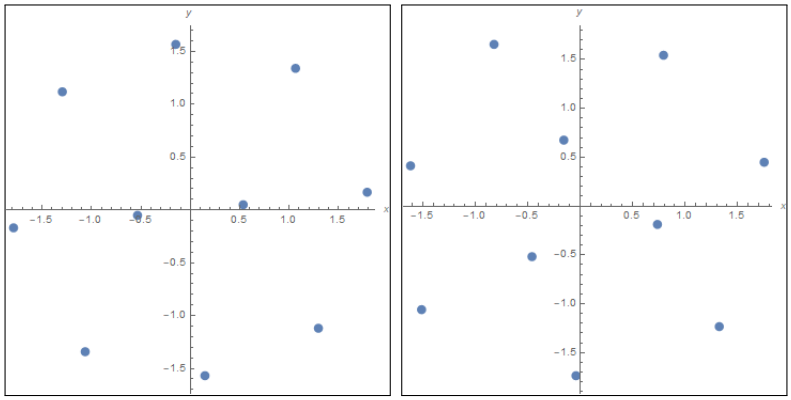

The 53 unstable structures that were found by the program detailed in Section 3.2 and subsequently analysed for the purposes of this work, they are arranged by energy, in increasing order, from E = 35.632424 to E = 46.691684.